Scaling forms of particle densities for Lévy walks and strong anomalous diffusion

Marco Dentz, Tanguy Le Borgne, Daniel R. Lester, Felipe P.J. de Barros

Scaling forms of particle densities for Lévy walks and strong anomalous diffusion

Marco Dentz[*]

Spanish National Research Council, IDAEA, CSIC, 08034 Barcelona, Spain

Tanguy Le Borgne

Geosciences Rennes, UMR No. 6118, Université de Rennes 1, CNRS, Rennes, France

Daniel R. Lester

School of Civil, Environmental and Chemical Engineering, RMIT University, 3000 Melbourne, Victoria, Australia

Felipe P. J. de Barros

Sonny Astani Department of Civil and Environmental Engineering, University of Southern California, 3620 S. Vermont Avenue, KAP 224B, Los Angeles, California 90089, USA

We study the scaling behavior of particle densities for Lévy walks whose transition length r is coupled with the transition time t as $|r| \propto t^\alpha$ with an exponent $\alpha > 0$. The transition-time distribution behaves as $\psi(t) \propto t^{-1-\beta}$ with $\beta > 0$. For $1 < \beta < 2\alpha$ and $\alpha \geqslant 1$, particle displacements are characterized by a finite transition time and confinement to $|r| < t^\alpha$ while the marginal distribution of transition lengths is heavy tailed. These characteristics give rise to the existence of two scaling forms for the particle density, one that is valid at particle displacements $|r| \ll t^\alpha$ and one at $|r| \lesssim t^\alpha$. As a consequence, the Lévy walk displays strong anomalous diffusion in the sense that the average absolute moments $\langle |r|^q \rangle$ scale as $t^{q\nu(q)}$ with $\nu(q)$ piecewise linear above and below a critical value q_c. We derive explicit expressions for the scaling forms of the particle densities and determine the scaling of the average absolute moments. We find that $\langle |r|^q \rangle \propto t^{q\alpha/\beta}$ for $q < q_c = \beta/\alpha$ and $\langle |r|^q \rangle \propto t^{1+\alpha q - \beta}$ for $q > q_c$. These results give insight into the possible origins of strong anomalous diffusion and anomalous behaviors in disordered systems in general.

　　　　PACS number(s): 05.40.Fb, 02.50.Ey, 05.60.−k

I. INTRODUCTION

Lévy walk dynamics of anomalous diffusion have been observed for transport in disordered systems as diverse as the transmission of light through optical media [1], dispersion in fluid turbulence [2], animal foraging behaviors [3], transport in strongly correlated velocity fields [4], dispersion in heterogeneous porous media [5], and dispersion in intermittent maps [6]; see also the recent review by Zaburdaev *et al.* [7]. Lévy walks can be seen as coupled continuous-time random walks (CTRWs) [8,9] characterized by heavy-tailed marginal distributions of the spatial transition length and transition time.

The coupling between transition length r and time t for a particle that moves with constant speed v between turning points is given by the kinematic relationship $r = vt$. The speed v may change randomly at the turning points [10,11]. This linear coupling model between transition length and times has been intensely studied in the literature [7,10–12] in terms of the first-passage times and displacement statistics. Recently it was found [11] that under certain conditions the spatial density is characterized by two scaling forms. One describes the bulk density for $|r| \ll vt$, while the other characterizes the tail behavior at vt. These two scaling forms explain the occurrence of strong anomalous diffusion in the linearly coupled Lévy walk.

A system can be characterized as exhibiting strong anomalous diffusion if the average absolute moments $\langle |r|^q \rangle$ scale

as $t^{q\nu(q)}$ with $\nu(2) > 1/2$ and $\nu(q)$ not a linear function of q [13]. This characteristic precludes the density from having a single scaling form, as is the case for an uncoupled CTRW characterized by a heavy-tailed (power-law) transition-time distribution $\psi(t)$ [14]. For the linearly coupled Lévy walk, anomalous diffusion is strong and the exponent $\nu(q)$ is a piecewise linear function of q. For q smaller than some critical value of $q_c = \beta$, the exponent $q\nu(q) = q/\beta$, while for $q > q_c$, it behaves as $q\nu(q) = 1 + q - \beta$ [11,14].

Here we consider the Lévy walk characterized by the nonlinear coupling [15–18]

$$|r| = t^\alpha \tag{1}$$

with $\alpha > 0$. Both r and t are understood to be dimensionless. This coupling model has been studied in terms of the scaling of the mean-square displacement $\langle r(t)^2 \rangle$ [16]. However, the scaling forms and scaling function for the spatial densities have not been known so far [7]. These scaling forms provide a complete characterization of the average transport behavior. Specifically, they allow one to determine the behavior of the average absolute moments $\langle |r(t)|^n \rangle$ and thus characterize the nature of anomalous diffusion.

In the next section we provide basic relations for the Lévy walk, which form the starting point for the derivation of the scaling forms for the particle densities in Sec. III. The analytical results are corroborated by numerical random-walk particle-tracking simulations. Section IV uses these results to determine the scaling of the average absolute moments. A summary is given and conclusions are made in Sec. V.

---

[*]marco.dentz@csic.es

II. LÉVY WALKS

We consider the $(d = 1)$-dimensional CTRW

$$r_{n+1} = r_n + \rho_n, \quad t_{n+1} = t_n + \tau_n. \quad (2)$$

The Lévy walk [15] couples the independent and identically distributed random space and time increments ρ_n and τ_n according to (1). They are characterized by the joint density function of transition length and times

$$\psi(\rho,\tau) = \frac{1}{2}\delta(|\rho| - \tau^\alpha)\psi(\tau), \quad (3)$$

where $\psi(\tau)$ is the distribution density of transition times τ_n. The joint density $\psi(\rho,\tau)$ and the transition-time density are distinguished by their arguments without ambiguity. Thus, the marginal density $\psi_r(\rho)$ of transition length ρ_n reads

$$\psi_r(\rho) = \frac{1}{2\alpha}|\rho|^{1/\alpha - 1}\psi(|\rho|^{1/\alpha}). \quad (4)$$

The CTRW (2) determines the particle positions $r(t)$ at time t as

$$r(t) = r_{n_t}, \quad n_t = \min(n|t_n \leqslant t), \quad (5)$$

where the renewal process n_t counts the number of steps needed to arrive at time t. Note that (5) considers the CTRW (2) in the waiting-time interpretation; τ_n is interpreted as the waiting time of a particle at a turning point r_n, which is assumed to be much longer than the time to make a transition to the next turning point.

Note that in the case $\alpha \geqslant 1$ in (1) we have

$$|r_n| \leqslant t_n^\alpha \quad (6)$$

as a result of the monotonicity of the norm. Thus, the particle positions $r(t) \leqslant t^\alpha$ and, accordingly, the particle densities have a sharp cutoff at t^α. For $\alpha < 1$, this is not the case. This property has an important impact on the nature of diffusion for values of α above or below 1 and the scaling properties of the particle densities as studied in detail below.

We consider a heavy-tailed transition-time density that behaves as

$$\psi(\tau) \propto \tau^{-1-\beta} \quad (7)$$

for $\tau \gg 1$ and $\beta > 0$. This gives for the marginal density $\psi_r(\rho)$ of transition length the heavy-tailed distribution

$$\psi_r(\rho) \propto |\rho|^{-1-\gamma}, \quad \gamma = \frac{\beta}{\alpha}. \quad (8)$$

Note that the uncoupled CTRW characterized by $\psi(\rho,\tau) = \psi_r(\rho)\psi(\tau)$ shows Lévy flightlike behavior for $0 < \gamma < 2$ in the sense that the moments $\langle |r(t)|^q \rangle$ for $q > \gamma$ do not exist (see also Ref. [7]). Here the coupling of transition length and time, and the resulting confinement (6) of the particle trajectory guarantee that all trajectory moments exist. The numerical random-walk simulations employed below to determine the particle densities use the explicit transition-time density

$$\psi(\tau) = \beta\tau^{-1-\beta}\gamma(1+\beta,\tau), \quad (9)$$

where $\gamma(a,x)$ is the lower incomplete gamma function [19]. This distribution decreases as the power law (7) for $\tau \gg 1$ and goes toward $\beta/(1+\beta)$ for $\tau \ll 1$.

The objective of this paper is to study the spatial aspects of the Lévy walk. In general, the particle density for the CTRW (2) is defined in terms of the particle trajectories $r(t) = r_{n_t}$ as

$$p(r,t) = \langle\delta(r - r_{n_t})\rangle. \quad (10)$$

The evolution of (10) is governed by the system of equations [9]

$$p(r,t) = \int_0^t dt' R(r,t') \int_{t-t'}^\infty d\tau\,\psi(\tau), \quad (11)$$

$$R(r,t) = \delta(t)\delta(r) + \int dr' R(r',t')\psi(r-r',t-t'), \quad (12)$$

where we set the initial particle positions $r_0 = 0$; $R(r,t)dr\,dt$ denotes the probability that a particle is in $[r,r+dr]$ and $[t,t+dt]$. This system of equations can be easily solved after performing a Fourier-Laplace transform. The particle density then reads [16]

$$p(k,\lambda) = \frac{1 - \psi(\lambda)}{\lambda}\frac{1}{1 - \psi(k,\lambda)}, \quad (13)$$

which is the starting point for the analysis presented in the next section. The Laplace transform in time is defined in Ref. [19] and the Laplace variable here is denoted by λ. For the Fourier transform and its inverse, we adopt the definition

$$p(k,t) = \int dr\,\exp(ikr)p(r,t), \quad (14)$$

$$p(r,t) = \int \frac{dk}{2\pi}\exp(-ikr)p(k,t), \quad (15)$$

where k is the wave number. Fourier and Laplace transformed quantities in the following are identified by their arguments.

III. SCALING FORMS

In order to derive scaling forms for the particle density $p(r,t)$, we start from its Fourier-Laplace transform (13), which is quantified in terms of the Laplace transform $\psi(\lambda)$ of the transition-time density and the Fourier-Laplace transform of the joined density $\psi(k,\lambda)$. The Fourier-Laplace transform transform of $\psi(\rho,\tau)$ given by (3) can be written as

$$\psi(k,\lambda) = \int_0^\infty dt\,\exp(-\lambda t)\cos(|k|t^\alpha)\psi(t). \quad (16)$$

We can write (16) in the form

$$\psi(k,\lambda) = \psi(\lambda) + \int_0^\infty dt\,\exp(-\lambda t)[\cos(|k|t^\alpha) - 1]\psi(t). \quad (17)$$

For $\lambda \ll 1$ and $n-1 < \beta < n$, $\psi(\lambda)$ can be approximated up to order λ^β by $\psi(\lambda) \approx \psi_a(\lambda)$ with

$$\psi_a(\lambda) = 1 + \sum_{i=1}^{n-1}(-1)^i a_i\lambda^i + (-1)^n a_\beta\lambda^\beta, \quad (18)$$

where the coefficients a_i and a_β are positive constants [20]. Notice that for $n > 1$, $a_1 = \tau_m = \langle\tau\rangle$ is equal to the mean transition time. The approximation (18) of the transition-time

probability density function (PDF) (9) and the corresponding coefficients a_i and a_β are derived in Appendix A 1.

In order to derive scaling forms for the particle densities, we distinguish the two cases of weak and strong coupling between the space and time increments. The weak coupling is characterized by $\gamma > 2$ in (8), or equivalently $\beta > 2\alpha$, which means that the marginal transition length distribution (8) has finite mean and variance. The strong-coupling case is characterized by a broad distribution of transition length, which corresponds to $\beta < 2\alpha$.

A. Weak coupling $\beta > 2\alpha$

For weak coupling transport is dispersive as discussed in Ref. [16]. For completeness, we briefly summarize the behavior of the particle densities in the weakly coupled limit. For $\beta > 1$, the mean transition time $\tau_m = \langle \tau \rangle < \infty$ is finite and the central limit theorem predicts normal transport.

The range $0 < \beta < 1$ implies that $\alpha < 1/2$. This means that particle displacements have an open range. The Laplace transform of the transition-time density here is given by (18) as

$$\psi_a(\lambda) = 1 - a_\beta \lambda^\beta. \tag{19}$$

We consider now the range $|r| \gg t^\alpha$ while $t \gg 1$, which corresponds to $k\lambda^{-\alpha} \ll 1$ while $\lambda \ll 1$. In this limit, we can expand (17) as

$$\psi(k,\lambda) = 1 - a_\beta \lambda^\beta - \frac{\langle \tau^{2\alpha} \rangle}{2} k^2 + \cdots, \tag{20}$$

where the dots denote subleading contributions. Notice that $\langle \tau^{2\alpha} \rangle < \infty$ because $\beta > 2\alpha$. Thus, in this limit, we obtain for the Fourier-Laplace transform (13) of the particle density

$$p(k,\lambda) \approx \frac{1}{\lambda} \frac{1}{1 + a_\beta^{-1} \langle \tau^{2\alpha} \rangle k^2 \lambda^{-\beta}}. \tag{21}$$

The inverse Fourier-Laplace transform of this expression can be written as

$$p(r,t) \approx \int_{-\infty}^{\infty} \frac{dk}{2\pi} \int_{\kappa-i\infty}^{\kappa+\infty} \frac{d\lambda}{2\pi i} \frac{1}{\lambda} \frac{\exp(\lambda t - ikr)}{1 + a_\beta^{-1} \langle \tau^{2\alpha} \rangle k^2 \lambda^{-\beta}}. \tag{22}$$

Rescaling $\lambda t \to \lambda$ and $kt^{\beta/2} \to k$ gives the single scaling form

$$p(r,t) \approx t^{-\beta/2} f_0\left(\frac{|r|}{t^{\beta/2}}\right). \tag{23}$$

The scaling function decreases exponentially fast for $|r| \gg t^{\beta/2}$.

B. Strong coupling $\beta < 2\alpha$

In the following, we focus on the more interesting case $\beta < 2\alpha$, which implies that $0 < \gamma < 2$ in (8). This means that the marginal density of transition lengths is heavy tailed. For $k \ll 1$, the Fourier transform of the spatial transition density (8) can then be approximated as [7]

$$\psi_r(k) = 1 - c_\gamma |k|^\gamma + \cdots, \tag{24}$$

where the dots denote subleading contributions. The constant $c_\gamma > 0$ is a constant determined by the specific shape of the transition length PDF $\psi_r(\rho)$ (see also Appendix A 2).

In order to derive scaling forms for the particle density, we write (17) in the form

$$\psi(k,\lambda)$$
$$= \psi(\lambda) + \lambda^{-1} \int_0^\infty dt \exp(-t)[\cos(|k|\lambda^{-\alpha}t^\alpha) - 1]\psi(t\lambda^{-1}). \tag{25}$$

For small $\lambda \ll 1$, we approximate $\psi(t\lambda^{-1}) \approx a_0 t^{-1-\beta}\lambda^{\beta-1}$ in order to obtain

$$\psi(k,\lambda) \approx \psi_a(\lambda) + \lambda^\beta F(|k|\lambda^{-\alpha}), \tag{26}$$

where $\psi_a(\lambda)$ is defined by (18) and a_0 is a constant that depends on the specific choice of $\psi(t)$; see Appendix A 1 for the explicit expressions for $\psi_a(\lambda)$ and the coefficient a_0 for the transition-time PDF (9). The function $F(k)$ is defined by

$$F(k) \equiv a_0 \int_0^\infty dt \exp(-t)[\cos(kt^\alpha) - 1]t^{-1-\beta}. \tag{27}$$

All the derivatives of $F(k)$ with respect to k exist due to the condition $\alpha > \beta/2$. In the limit $k \ll 1$, we have

$$F(k) = -c_2 k^2 + \cdots. \tag{28}$$

The dots denote subleading contributions of order k^4.

Note that setting $\lambda = 0$ in $\psi(k,\lambda)$ gives the Fourier transform $\psi_r(k)$ of the marginal density (8), which can be approximated by (24). This implies that $F(|k|\lambda^{-\alpha})$ behaves for finite k and in the limit $\lambda \to 0$ as

$$F(|k|\lambda^{-\alpha}) \approx -c_\gamma |k|^\gamma \lambda^{-\beta}. \tag{29}$$

Using (26) for $\lambda \ll 1$, the Fourier-Laplace transform of the spatial density can now be written in the form

$$p(k,\lambda) \approx \frac{1 - \psi_a(\lambda)}{\lambda} \frac{1}{1 - \psi_a(\lambda) - \lambda^\beta F(|k|\lambda^{-\alpha})}. \tag{30}$$

This expression is the basis for the derivation of the scaling forms of the spatial density $p(r,t)$ for different ranges of $\beta > 0$ presented in the following.

We distinguish two cases. First, we consider $\alpha \geqslant 1$, which corresponds to a compact displacement range because of $|r(t)| \leqslant t^\alpha$ as indicated by (6). Second, we study the case $\alpha < 1$ for which the displacement range is open.

1. Compact displacement range $\alpha \geqslant 1$

We distinguish between the β ranges $0 < \beta < 1$ and $\beta > 2$. In the first case, the mean transition time τ_m is not finite. In the second case $\tau_m < \infty$. This has an impact on the scaling behavior as detailed below.

a. Infinite mean transition time $0 < \beta < 1$. In this β range the Laplace transform $\psi(\lambda)$ of the transition-time density can be approximated by (19). Inserting (19) into (30), we obtain for the Fourier-Laplace transform $p(k,\lambda)$ of the particle density

$$p(k,\lambda) \approx \frac{1}{\lambda} \frac{1}{1 - a_\beta^{-1} F(|k|\lambda^{-\alpha})}. \tag{31}$$

As above, we write down the inverse Fourier and Laplace transforms of this expression as

$$p(k,\lambda) \approx \int_{-\infty}^{\infty} \frac{dk}{2\pi} \int_{\kappa-i\infty}^{\kappa+\infty} \frac{d\lambda}{2\pi i} \frac{1}{\lambda} \frac{\exp(\lambda t - ikr)}{1 - a_\beta^{-1} F(|k|\lambda^{-\alpha})}. \tag{32}$$

Rescaling $\lambda t \to \lambda$ and $k t^\alpha \to k$ gives the single scaling form

$$p(r,t) \approx t^{-\alpha} f_1 \left(\frac{|r|}{t^\alpha} \right), \tag{33}$$

with $f_1(r)$ a scaling function that is discussed below. Note that this scaling form is also valid in the case of an open displacement range for $\alpha < 1$.

In order to derive explicit expressions for the scaling function $f_1(r)$ we first consider the bulk density at $|r| \ll t^\alpha$, which corresponds to $|k|\lambda^{-\alpha} \gg 1$. In this limit, we can approximate (31) as

$$p(k,\lambda) \approx \frac{a_\beta}{c_\gamma} \lambda^{-1} (|k|\lambda^{-\alpha})^{-\beta/\alpha}, \tag{34}$$

where we used (29) and set $\gamma = \beta/\alpha$. The inverse Fourier-Laplace transform gives for the scaling function $f_1(r)$ the explicit expression

$$f_1(r) \propto r^{\beta/\alpha - 1}. \tag{35}$$

The density is cut off here at $|r| = t^\alpha$ as indicated by (6). We can identify the form of this cutoff by considering the case $|k|\lambda^{-\alpha} \sim 1$, which corresponds to $|r| \sim t^\alpha$. In this case, we approximate (31) by

$$p(k,\lambda) \approx \lambda^{-1} + a_\beta^{-1} \lambda^{-1} F(|k|\lambda^{-\alpha}). \tag{36}$$

The inverse Fourier-Laplace transform of the expression on the right-hand side of (36) can be performed explicitly by using (27). This gives for the scaling function $f_1(r)$ for $|r| > 0$

$$f_1(r) = \frac{a_0}{2 a_\beta \alpha \Gamma(\beta)} (1 - r^{1/\alpha})^\beta r^{-1-\beta/\alpha} H(1-r), \tag{37}$$

with $H(r)$ the Heaviside step function (see also Appendix B).

Figure 1 shows particle densities obtained by numerical random-walk particle-tracking simulations based on (2). The densities are rescaled to highlight the general scaling form (33), which is confirmed for $t \gg 1$. The solid lines illustrate the explicit expressions (35) and (37) for the scaling function
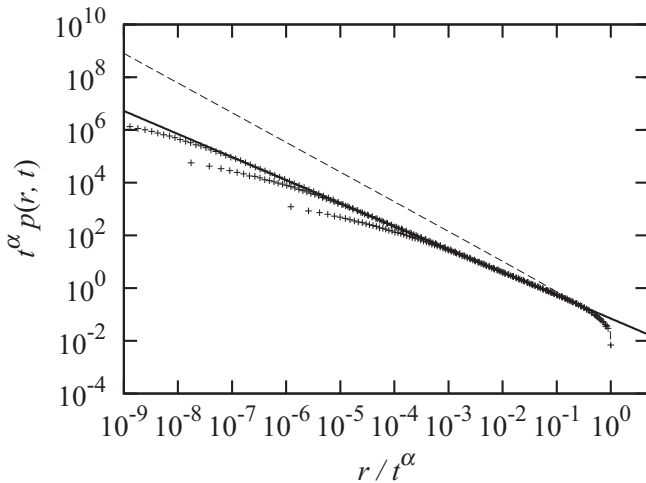

FIG. 1. Particle densities $p(r,t)$ at times (from top to bottom) $t = 10^2$, 10^3, and 10^4 for $\alpha = 2$ and $\beta = 1/4$. The symbols denote random-walk simulations using 10^6 particles and the solid lines denote the scaling forms (solid) (35) and (dashed) (37).

$f_1(r)$. Note that (37) merely captures the sharp cutoff, while (35) describes the power-law decrease at large times.

b. Finite mean transition time $\beta > 1$. In this β range, $\psi_a(\lambda)$ is given by (18) for $n = \lceil 2\alpha \rceil$, where the upper braces denote the ceiling function. The particle density then can be approximated as

$$p(k,\lambda) \approx \frac{\tau_m}{\tau_m \lambda + G_\beta(\lambda) - \lambda^\beta F(|k|\lambda^{-\alpha})}, \tag{38}$$

where we define $G_\beta(\lambda) = 1 - \psi_a(\lambda) - \lambda \tau_m$; $F(k)$ is defined in (27). Recall that $\tau_m = \langle \tau \rangle$ is the mean transition time.

Again recall that we consider the case $\alpha \geqslant 1$, which implies that $|r(t)| \leqslant t^\alpha$; this means that the density is cut off at t^α. We explore now the behaviors of $p(r,t)$ at $|r| \ll t^\alpha$ and for distances close to the cutoff $|r| \lesssim t^\alpha$.

In the limit $\lambda \ll 1$ and $|k|\lambda^{-\alpha} \gg 1$, which corresponds to $|r| \ll t^\alpha$ while $t \gg 1$, we use expression (29) in order to obtain the following approximation for $p(k,\lambda)$:

$$p(k,\lambda) \approx \frac{\tau_m}{\tau_m \lambda + c_\gamma |k|^\gamma}. \tag{39}$$

Its inverse Laplace transform gives

$$p(k,t) \approx \exp(-c_\gamma |k|^\gamma t/\tau_m), \tag{40}$$

which is the Fourier representation of the symmetric Lévy stable density with the stability parameter γ and the scale parameter c_γ/τ_m. Thus, we obtain for the bulk density $p(r,t)$ at $|r| \ll t^\alpha$ the scaling behavior

$$p(r,t) \approx t^{-1/\gamma} K_\gamma \left(\frac{r}{t^{1/\gamma}} \right), \tag{41}$$

where $K_\gamma(r)$ is the symmetric Lévy stable density. Recall that $\gamma = \beta/\alpha$.

We now consider the scaling of $p(r,t)$ at large times in the vicinity of the sharp cut off $|r| \lesssim t^\alpha$. This corresponds to $\lambda \ll 1$ while $|k|\lambda^{-\alpha}$ is of order 1. Thus, we can approximate (38) as

$$p(k,\lambda) \approx \frac{1}{\lambda} \left[1 - \frac{G_\beta(\lambda)}{\lambda \tau_m} \right] + \frac{\lambda^{\beta-2}}{\tau_m} F(|k|\lambda^{-\alpha}). \tag{42}$$

Note that $G_\beta(\lambda)/\lambda$ is of order $\lambda^{\beta-1}$ for $1 < \beta < 2$ and of order λ for $\beta > 2$. The inverse Fourier-Laplace transform of (42) gives for $|r| \neq 0$ the scaling form

$$p(r,t) \approx t^{1-\alpha-\beta} f_2 \left(\frac{|r|}{t^\alpha} \right), \tag{43}$$

which can be checked by inspection. Appendix B derives the following explicit expression for the scaling function $f_2(r)$:

$$f_2(r) = \frac{a_0}{\alpha \tau_m} (1 - r^{1/\alpha}) r^{-1-\gamma} H(1-r). \tag{44}$$

Note that for $r \ll 1$, the scaling function $f_2(r)$ displays the same power-law behavior proportional to $r^{-1-\gamma}$ as the Levy stable density in (41).

Figure 2 illustrates particle densities obtained from random-walk particle-tracking simulations using (2). The top figure emphasizes the scaling form (41) by scaling the data according by $t^{\alpha/\beta}$. The middle figure shows the same data set rescaled according to (43) in order to demonstrate the scaling form. The solid line depicts the scaling function (44). The bottom figure illustrates the scaling form (43) for different values of β.
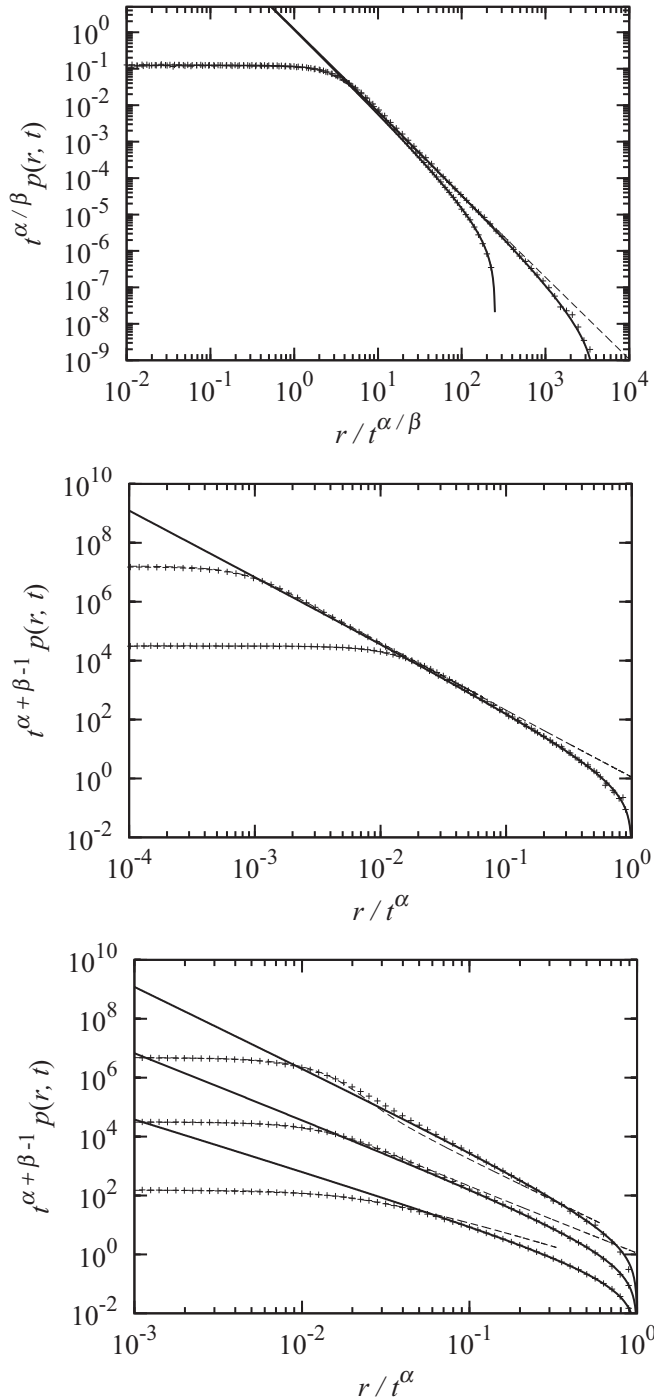
FIG. 2. The top and middle plots show particle densities $p(r,t)$ for $\alpha = 2$ and $\beta = 5/2$ at (from left to right) times $t = 10^2$ and 10^3. The symbols denote the data from the random-walk simulations using 10^7 particles and the lines the scaling forms (dashed) (41) and (solid) (43). Note that the crossover between the two scaling forms is marked by $r = r_c(t) \sim t^{\alpha/\beta}$. The bottom panel shows article densities $p(r,t)$ at time $t = 10^2$ for $\alpha = 2$ and (from top to bottom) $\beta = 7/2, 5/2,$ and $3/2$.

The crossover between the two scaling forms (41) and (43) is marked by the distance $|r_c| \propto t^{1/\gamma}$, which is the scale on which the Levy stable density (41) crosses over from the plateau to the power-law decay $r^{-1-\gamma}$, as illustrated in the top figure in

Fig. 2. This behavior and the existence of two scaling forms, one for the bulk density and one for the tails is in line with the observations in Ref. [11], who considered the linearly coupled Lévy walk, this means here $\alpha = 1$.

2. Open displacement range $\alpha < 1$

Unlike for $\alpha \geqslant 1$, here the density is not sharply cut off at the maximum absolute displacement $|r| = t^\alpha$. As a consequence, the particle densities are characterized by a single scaling form, whose Fourier-Laplace transforms can by found in Ref. [16]. For completeness we discuss them briefly in the following.

a. Infinite mean transition time $0 < \beta < 1$. We have seen in the previous section that for the range $0 < \beta < 1$, the particle density has the scaling form (33). The scaling function here is different. For $t \gg 1$ and $|r| > t^\alpha$, which corresponds to $\lambda \ll 1$ and $k\lambda^{-\alpha}$, we obtain by using (28) in (31) the approximation [16]

$$p(k,\lambda) \approx \frac{1}{\lambda} \frac{1}{1 + a_\beta^{-1} c_2 (k\lambda^{-\alpha})^2}. \tag{45}$$

This means that $p(r,t)$ decreases exponentially fast for $|r| \gg t^\alpha$.

b. Finite mean transition time $\beta > 1$. In order to derive the scaling form for the case with finite mean transition time, we use (28) in (38), which gives for the Fourier-Laplace transform of the particle density [16]

$$p(k,\lambda) \approx \frac{\lambda^{-1}}{1 + \lambda^{\beta - 2\alpha - 1} c_2 k^2 / \tau_m}. \tag{46}$$

The inverse Fourier-Laplace transform immediately gives the dispersive scaling form

$$p(r,t) \approx t^{-\nu} f_3\left(\frac{|r|}{t^\nu}\right), \quad \nu = (1 + 2\alpha - \beta)/2. \tag{47}$$

The scaling function decreases exponentially fast for $|r| \gg t^\nu$.

IV. AVERAGE ABSOLUTE MOMENTS

The average absolute moments are defined by

$$\langle |r(t)|^q \rangle = \int dr \, |r|^q \, p(r,t). \tag{48}$$

The scaling forms presented in the previous section allow for the systematic study of the behavior of the average absolute moments of all orders q.

A. Weak coupling $\beta > 2\alpha$

For $\beta > 1$, this means for $\tau_m < \infty$ that the central limit theorem implies normal diffusive transport and the average absolute moments scale as

$$\langle |r(t)|^q \rangle \propto t^{q/2}. \tag{49}$$

For $0 < \beta < 1$, we obtain, by using the scaling form (23) in (48), the scaling for the absolute displacement moments

$$\langle |r(t)|^q \rangle \propto t^{q\beta/2}, \tag{50}$$

which is of course the same as for an uncoupled CTRW. For weak coupling, anomalous diffusion is weak.

B. Strong coupling $\beta < 2\alpha$

We found in Sec. III that there is a single scaling form for the particle density for $0 < \beta < 1$. Thus, anomalous diffusion is also weak and the average absolute moments scale ballistically as

$$\langle |r(t)|^q \rangle \propto t^{q\alpha}, \tag{51}$$

where we used (33) in (48).

For $\beta > 1$ and an open displacement range, this means for $\alpha < 1$, the particle density is characterized by the single scaling form (47). Using this expression in (48), we obtain the dispersive scaling

$$\langle |r(t)|^q \rangle \propto t^{q\nu/2}, \quad \nu = (1 + 2\alpha - \beta)/2. \tag{52}$$

Anomalous diffusion is also weak.

This is very different for a compact displacement range $\alpha \geqslant 1$ and a finite mean transition time $\tau_m < \infty$, which means for $\beta > 1$. As discussed in Sec. III, in this case the particle density is characterized by two scaling forms: one that describes the bulk density and one that describes the behavior close to the sharp cutoff at $|r| = t^\alpha$.

We use now the scaling forms (41) for $|r| < r_c(t)$ and (43) for $|r| > r_c(t)$ in the definition (48) of the average absolute moments. This yields, after rescaling the integration variables, the expression

$$\langle |r(t)|^q \rangle = t^{q/\gamma} 2 \int_0^1 dr |r|^q K_\gamma(r)$$
$$+ t^{1+q\alpha-\beta} \int_0^\infty dr |r|^q f_2(r). \tag{53}$$

This means that for $q < \beta/\alpha$ the first term dominates and we have the scaling

$$\langle |r(t)|^q \rangle \propto t^{q\alpha/\beta}, \tag{54}$$

where we used that $\gamma = \beta/\alpha$. For $q = \gamma = \beta/\alpha$ both contributions are equally important such that $\langle |r(t)|^{\beta/\alpha} \rangle \propto t$. For

$q > \beta/\alpha$ the second term dominates such that

$$\langle |r(t)|^q \rangle \propto t^{1+\alpha q-\beta}. \tag{55}$$

Thus, anomalous diffusion is strong according to [13]. Figure 3 illustrates the α and β regions of normal, weak anomalous, and strong anomalous diffusion.

V. SUMMARY AND CONCLUSIONS

We studied the spatial characteristics of Lévy walks that are characterized by a general nonlinear coupling between transition length and time through $|r| = t^\alpha$ with $\alpha > 0$. The transition times are characterized by the heavy-tailed distribution $\psi(t) \propto t^{-1-\beta}$ with $\beta > 0$. We do not consider the marginal cases of integer β, which give rise to logarithmic terms in the average absolute displacements.

The spatial characteristics of anomalous diffusion are studied in terms of the scaling forms of the particle densities and average absolute displacements. It has been previously found [11,14] that the Lévy walk for $\alpha = 1$, which means linear coupling, and $1 < \beta < 2$ exhibits strong anomalous diffusion. This property has been traced back to the existence of two scaling forms of the particle density, one of which is valid for short displacement and the other one describes the density for long particle excursions. For low orders q of the moments $\langle |r|^q \rangle$ of the absolute displacement, the center of the particle density dominates the dispersion behavior, while for increasing q weight is shifted towards the tails and the second scaling form dominates the dispersion behavior.

We determined the scaling forms of the particle density for general $\alpha > 0$ and $\beta > 0$. For $0 < \beta < 1$ and $\beta > 2\alpha$ transport is dispersive [16], which means that $\langle |r|^q \rangle \propto t^{q\beta/2}$. In this region, the transition length and time are only weakly coupled. In fact, the marginal density of transition lengths is characterized by a finite variance. The particle density is characterized by a single scaling form, which is of the same type as the one for an uncoupled CTRW.

In the strongly coupled case ($\beta < 2\alpha$) the marginal density $\psi_r(r)$ is heavy tailed and characterized by the exponent $\gamma = \beta/\alpha < 2$. Nevertheless, for $0 < \beta < 1$ and for an open displacement range ($\alpha < 1$) we obtain a single scaling form for the particle density. For $0 < \beta < 1$, diffusion is dominated by a long spatial transition characterized by a large transition time. This gives rise to ballistic behavior and consequently the particle density is characterized by a single scaling form. For $\alpha < 1$ the coupling is not strong enough to confine the displacements. In both cases anomalous diffusion is weak.

Strong anomalous diffusion is only observed in the parameter region $1 < \beta < 2\alpha$ and a compact displacement range ($\alpha \geqslant 1$). This means that the Lévy walk here is characterized by a finite mean transition time $\tau_m < \infty$ and confinement to $|r(t)| \leqslant t^\alpha$. These properties give rise to the existence of two scaling forms for the particle density. The bulk of the density is characterized by a Lévy stable distribution of order β/α, which reflects the fact the marginal distribution of transition lengths is heavy tailed. At large distances, however, the particle displacements and thus densities are cut off due to the strong coupling of transition lengths and times. The cutoff behavior on the characteristic scale t^α is characterized by the scaling form $p(r,t) \sim t^{1-\alpha-\beta} f_2(|r|/t^\alpha)$. For $\alpha > 1$ we observe strong
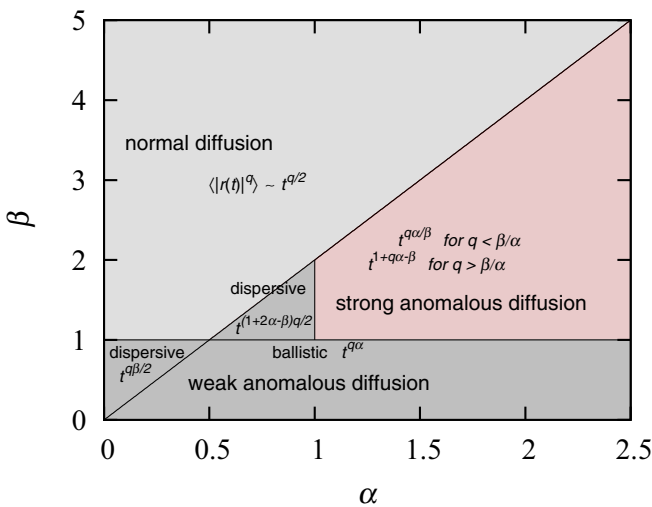

FIG. 3. (Color online) Illustration of the diffusion regimes depending on the coupling exponent α and the exponent β of the heavy-tailed transition-time distribution.

anomalous diffusion in parameter ranges of β for which both the mean and variance of the transition time are finite. Even though a mean transition time and its variance exist, meaning that the temporal transitions may be characterized by a single scale, the CTRW cannot be decoupled. These results shed light on anomalous diffusive behaviors observed in disordered systems and the possible origins of strong anomalous diffusion.

APPENDIX A: ASYMPTOTIC EXPANSIONS

1. Transition-time density

We detail here the expansion (18) of the Laplace transform of (9) for $\lambda \ll 1$. First, we notice that (9) can be written as

$$\psi(\tau) = \int_1^\infty dx \beta x^{-1-\beta} \frac{\exp(-\tau/x)}{x}. \tag{A1}$$

The Laplace transform of the latter reads

$$\psi(\lambda) = \int_1^\infty dx \beta x^{-1-\beta} \frac{1}{1+\lambda x}. \tag{A2}$$

For $n-1 < \beta < n$, we expand the integrand using the geometric sum as

$$\psi(\lambda) = 1 + \sum_{j=1}^{n-1} (-1)^j \lambda^j \beta \int_1^\infty dx\, x^{j-1-\beta} + (-1)^n \lambda^\beta \beta \int_1^\infty dx \frac{\lambda^{n-\beta} x^{n-1-\beta}}{1+\lambda x}. \tag{A3}$$

Rescaling $\lambda x \to x$ in the last integral gives

$$\psi(\lambda) = 1 + \sum_{j=1}^{n-1} (-1)^j \lambda^j \beta \int_1^\infty dx\, x^{j-1-\beta} + (-1)^n \lambda^\beta \beta \int_0^\infty dx \frac{x^{n-1-\beta}}{1+x} + \cdots, \tag{A4}$$

where the dots denote subleading contributions. Thus, the coefficients a_j and a_β in (18) are given by

$$a_j = \beta \int_1^\infty dx\, x^{j-1-\beta} = \frac{\beta}{\beta - j}, \tag{A5}$$

$$a_\beta = \beta \int_0^\infty dx \frac{x^{n-1-\beta}}{1+x} = \beta \mathrm{B}(n-\beta, 1+\beta-n), \tag{A6}$$

where $\mathrm{B}(\alpha, \beta)$ is the Beta function [19]. Furthermore, the constant a_0 that determines the asymptotic behavior of $\psi(\tau)$ for $\tau \gg 1$ is given by

$$a_0 = \beta \Gamma(1+\beta). \tag{A7}$$

2. Transition length density

We detail here the expansion of the Fourier transform of (8) for the specific transition-time PDF (9). The transition length

PDF $\psi_r(\rho)$ is obtained by inserting (9) into (8) as

$$\psi_r(\rho) = \frac{\beta}{2\alpha} |\rho|^{-1-\gamma} \gamma(1+\beta, |\rho|^{1/\alpha}). \tag{A8}$$

For $|\rho| \gg 1$, it can be approximated by

$$\psi_r(\rho) = \frac{\beta \Gamma(1+\beta)}{2\alpha} |\rho|^{-1-\gamma}. \tag{A9}$$

The Fourier transform of $\psi_r(\rho)$ can be approximated by

$$\psi_r(k) \approx \frac{\beta}{\alpha} \int_0^{r_0} dr \cos(kr) r^{-1-\gamma} \gamma(1+\beta, r^{1/\alpha}) + \frac{\beta \Gamma(1+\beta)}{\alpha} \int_{r_0}^\infty dr \cos(kr) r^{-1-\gamma}, \tag{A10}$$

where $r_0 \gg 1$. For $0 < \gamma < 1$ partial integration of the second integral on the right-hand side gives for $|k| \ll 1$ in leading order

$$\psi_r(k) \approx 1 - \Gamma(1-\gamma)\Gamma(1+\beta) \sin\left[\frac{(1-\gamma)\pi}{2}\right] |k|^\gamma. \tag{A11}$$

For $1 < \gamma < 2$, two integrations by parts and considering $|k| \ll 1$ gives in leading order

$$\psi_r(k) \approx 1 - \frac{\Gamma(2-\gamma)\Gamma(1+\beta)\cos[(2-\gamma)\pi/2]}{\gamma - 1} |k|^\gamma. \tag{A12}$$

These expressions define the constant c_γ.

APPENDIX B: SCALING FUNCTIONS

The scaling function (37) can be obtained by the inverse Fourier-Laplace transform of $g_1(k,\lambda) = \lambda^{-1} F(|k|\lambda^{-\alpha})$. Using the explicit form (27) of $F(k)$, we can write after rescaling the integration variable

$$g_1(k,\lambda) = a_0 \lambda^{-1-\beta} \int_0^\infty dt \exp(-\lambda t)[\cos(kt^\alpha) - 1] t^{-1-\beta}. \tag{B1}$$

The inverse Fourier transform gives immediately

$$g_1(r,\lambda) = a_0 \lambda^{-1-\beta} \int_0^\infty dt \exp(-\lambda t)\left[\tfrac{1}{2}\delta(|r|-t^\alpha) - \delta(r)\right] t^{-1-\beta}. \tag{B2}$$

We consider the case $|r| > 0$ and disregard the second term in square brackets. Performing now the inverse Laplace transform gives the expression

$$g_1(r,t) = a_0 \int_0^t dt' \frac{(t-t')^\beta}{2\Gamma(1+\beta)} \delta(|r| - t'^\alpha) t'^{-1-\beta}. \tag{B3}$$

Executing the integral gives the expression

$$g_1(r,t) = a_0 \frac{(t-|r|^{1/\alpha})^\beta}{2\alpha\Gamma(1+\beta)} |r|^{-1-\beta/\alpha} H(t^\alpha - |r|), \tag{B4}$$

which yields the scaling function (37).

The derivation of the scaling function (43) is analogous. We consider the inverse Fourier-Laplace transform of $g_2(k,\lambda) = \lambda^{\beta-2} F(|k|\lambda^{-\alpha})$. Using (27) and again rescaling the integration variable gives the expression

$$g_2(k,\lambda) = a_0 \lambda^{-2} \int_0^\infty dt \exp(-\lambda t)[\cos(kt^\alpha) - 1]t^{-1-\beta}.$$

$$\text{(B5)}$$

Performing the inverse Fourier and Laplace transforms, we obtain, by using the same steps as above,

$$g_2(r,t) = \frac{a_0}{2} \int_0^t dt'(t - t')\delta(|r| - t'^\alpha)t'^{-1-\beta}.$$

$$\text{(B6)}$$

The remaining integration gives

$$g_2(r,t) = \frac{a_0}{2\alpha}(t - |r|^{1/\alpha})|r|^{-1-\beta/\alpha}H(t^\alpha - |r|),$$

$$\text{(B7)}$$

which yields the scaling function (44).

[1] P. Barthelemy, J. Bertolotti, and D. S. Wiersma, Nature (London) **453**, 495 (2008).

[2] M. F. Shlesinger, B. J. West, and J. Klafter, Phys. Rev. Lett. **58**, 1100 (1987).

[3] A. M. Reynolds and C. J. Rhodes, Ecology **90**, 877 (2009).

[4] M. Dentz and D. Bolster, Phys. Rev. Lett. **105**, 244301 (2010).

[5] B. Berkowitz, A. Cortis, M. Dentz, and H. Scher, Rev. Geophys. **44**, RG2003 (2006).

[6] G. Zumofen, J. Klafter, and A. Blumen, Phys. Rev. E **47**, 2183 (1993).

[7] V. Zaburdaev, S. Denisov, and J. Klafter, Rev. Mod. Phys. **87**, 483 (2015).

[8] E. W. Montroll and G. H. Weiss, J. Math. Phys. **6**, 167 (1965).

[9] H. Scher and M. Lax, Phys. Rev. B **7**, 4491 (1973).

[10] M. Dentz, H. Scher, D. Holder, and B. Berkowitz, Phys. Rev. E **78**, 041110 (2008).

[11] A. Rebenshtok, S. Denisov, P. Hänggi, and E. Barkai, Phys. Rev. E **90**, 062135 (2014).

[12] D. Froemberg, M. Schmiedeberg, E. Barkai, and V. Zaburdaev, Phys. Rev. E **91**, 022131 (2015).

[13] P. Castiglione, A. Mazzino, P. Muratore-Ginanneschi, and A. Vulpiani, Physica D **134**, 75 (1999).

[14] K. H. Andersen, P. Castiglione, A. Mazzino, and A. Vulpiani, Eur. Phys. J. B **18**, 447 (2000).

[15] J. Klafter, A. Blumen, G. Zumofen, and M. F. Shlesinger, Phys. A **168**, 637 (1990).

[16] J. Klafter, A. Blumen, and M. F. Shlesinger, Phys. Rev. A **35**, 3081 (1987).

[17] T. Akimoto and T. Miyaguchi, Phys. Rev. E **87**, 062134 (2013).

[18] T. Akimoto and T. Miyaguchi, J. Stat. Phys. **157**, 515 (2014).

[19] M. Abramowitz and I. A. Stegun, *Handbook of Mathematical Functions* (Dover, New York, 1972).

[20] M. Dentz, A. Cortis, H. Scher, and B. Berkowitz, Adv. Water Resour. **27**, 155 (2004).